Combustion Generated Nanoparticles Smaller and Larger than 10 nm

L. A. Sgro[1], L. Speranza[2], A. C. Barone[1], B. Borghese[2], P. Minutolo[3], A. D'Anna[1], A. D'Alessio[1], G.Lanzuolo[1]

[1]Università 'Federico II' Napoli, [2]Istituto Motori, CNR, [3]Istituto Ricerche sulla Combustione, CNR

Abstract

Using various diagnostics with high sensitivity in the 1-5 nm size range, some of which we are modifying to be sensitive in this size range, we are working to determine the size and concentration of inception particles formed in the combustion of hydrocarbons. We compare *in situ* and *extra situ* sampling methods since sampling nanoparticles can change the size distribution by losses, coagulation and/or condensation or interactions with the sampling medium. To examine the particles formed in fuel rich hydrocarbon combustion, we compare size distributions determined by in situ UV-visible optical measurements, atomic force microscopy (AFM) analysis of thermophoretic samples, and various sizing methods applied to water samples collected from premixed flames and four last generation engine exhausts. Some combustion conditions generate both soot and nanosize organic carbon (or NOC) particles, and others produce only NOC particles. Previous work shows that 2 main types of primary particles are formed in rich hydrocarbon combustion, including soot and NOC particles. Soot particles are hydrophobic, graphitic, 10-50 nm in size, absorb visible light, and grow by coagulation into aggregates while NOC particles are an order of magnitude smaller, can be trapped in water samples, do not absorb visible light and do not coagulate readily in flames, even in high concentrations. Water sampling appears to be a method for isolating NOC particles from the more graphitic and hydrophobic soot particles. Concentrating water samples containing NOC by evaporation increases the signal:noise and certainty in some of the measurement techniques without affecting the size distribution measured. Slight differences are noted in the size determination of NOC particles in water samples and the size of NOC particles dried by electrospray, which may provide a measure of the layer of water attached to the particles in the hydrosols or the particles affinity for water. Since some of the techniques used are modified commercial instruments, we also show their sensitivity and ability to determine size using molecular standards in the size range of 1-5 nm. Comparing the concentration of NOC particles evaluated by different measurement techniques indicates that NOC particles constitute 75-90 % of the total organic carbon in the samples after concentration by evaporation. The agreement in concentration between total organic carbon and NOC concentration determined by UV-visible extinction in the water samples suggests that the UV-visible extinction can be used to estimate the *in situ* concentration of NOC particles when the NOC signature spectra is apparent after subtracting other absorbing species present, as is demonstrated with measurements in diluted engine exhausts. Because of their small size NOC particles have a higher kinetic energy than soot particles, which is noted experimentally by their relatively lower coagulation rate with other particles and adhesion or sticking efficiency to substrates in thermophoretic sampling. As a result, AFM measurements show the size range of particles present, including both NOC and soot particles, but the strongly size dependent sticking efficiency of the particles to the substrate must be taken into account to determine size distributions from thermophoretically collected samples. As has been done for particle coagulation rate, the sticking efficiency for both NOC and soot particles on Mica substrates can be modelled within the framework of the kinetic gas theory to determine the original size distribution from AFM measurements. The calculated size distribution is shifted towards smaller particles, and agrees well with *in situ* particle size distributions elaborated from optical measurements in laboratory flames.

Particle Measurement and Collection of Water Samples

In situ

UV-visible optical techniques

light scattering / absorption

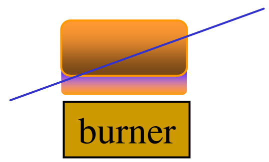

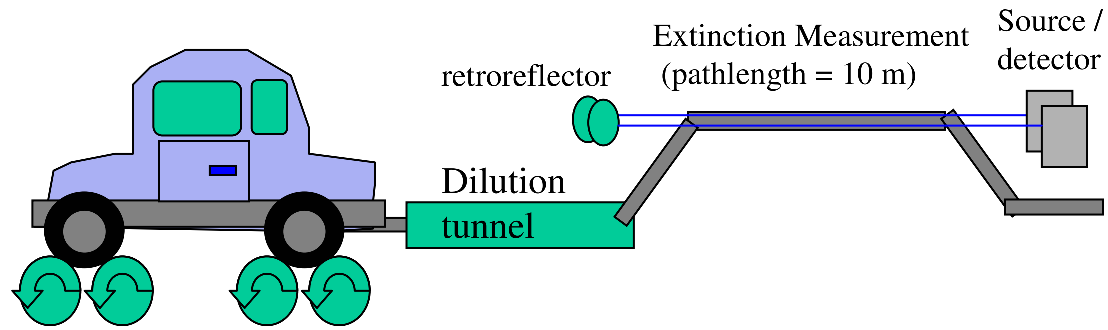

Dynamometer – New European Driving Cycle (NEDC)

High temperature thermophoretic sampling

Atomic Force Microscopy

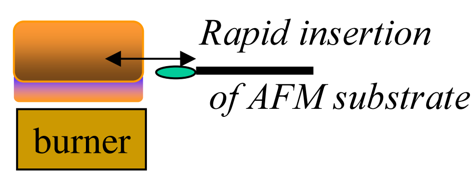

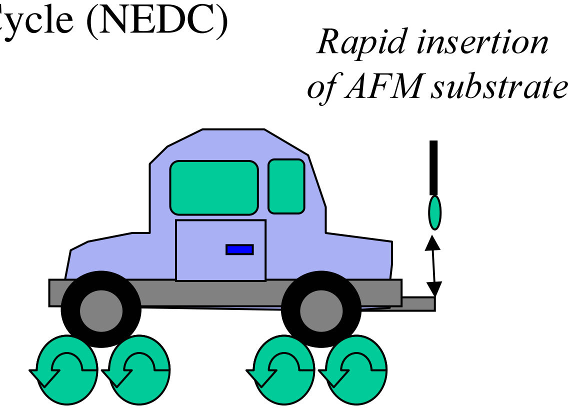

Dynamometer

Extra situ water samples

Electrospray-NanoDMA (E-DMA) and Dynamic light scattering (DLS)

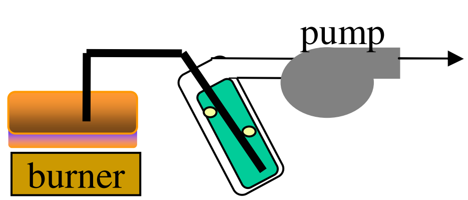

Water sample

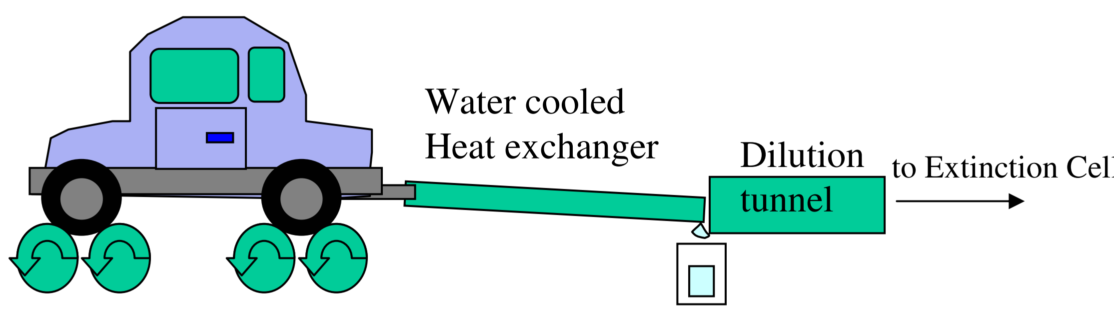

Dynamometer

Water sample

In situ /High Temperature Measurements

Optical Measurements

Combined Extinction-Scattering measurements give a mean particle diameter
(weighted toward larger particles in bimodal distibutions)

$$d_{ext-scat} = \sqrt[3]{\frac{\sum_i N_i d_i^6}{\sum_i N_i d_i^3}}$$

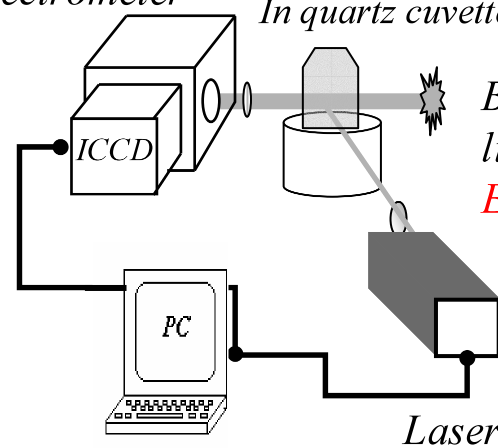

Measuring the UV-visible Extinction spectra gives the relative amounts of NOC and soot particles[2]

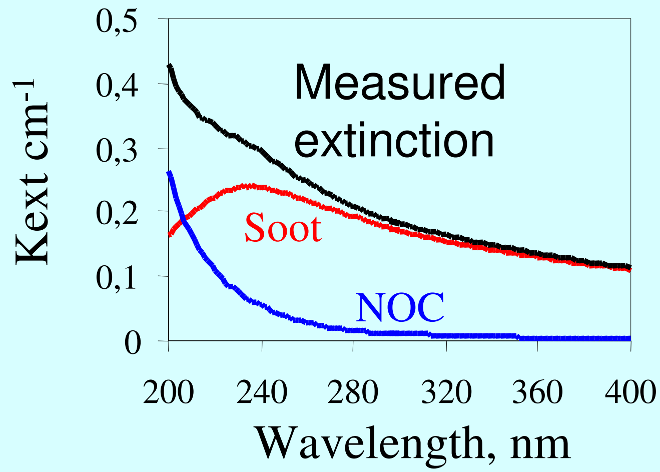

Size Analysis of water samples: DLS and E-DMA

Dynamic Light Scattering (DLS)

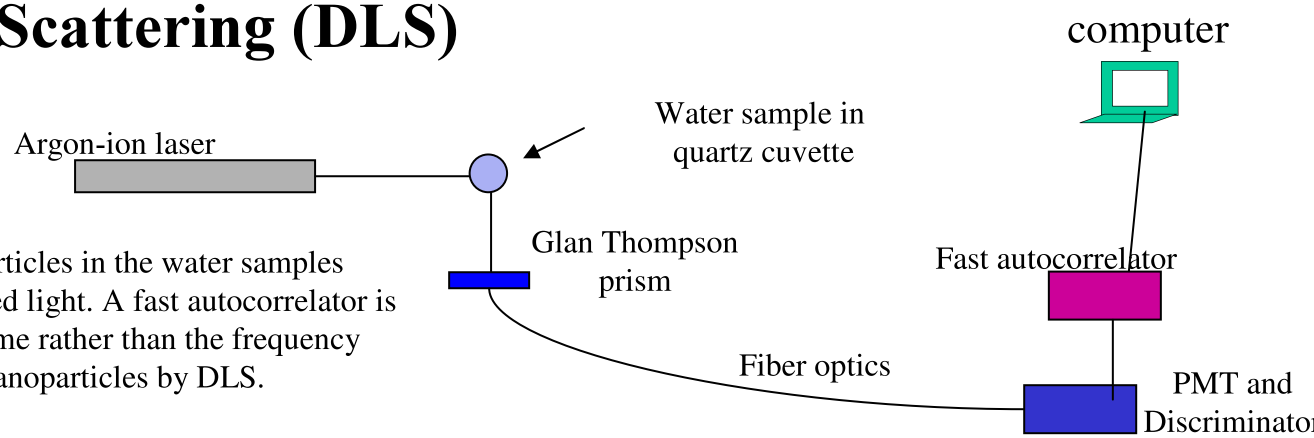

Diffusion or Brownian motion of the particles in the water samples causes a slight fluctuation in the scattered light. A fast autocorrelator is used to measure the fluctuation in the time rather than the frequency domain, allowing the measurement of nanoparticles by DLS.

Electrospray – Differential Mobility Analysis (E-DMA)

dry & charge particles contained in water samples – measures the size distribution of dried, charged particles entrained in a gas flow

Detector: Condensation Particle Counter (CPC) grows particles to a detectable size & counts them

Electrospray produces highly charged droplets ($D_{droplet}$ = 100 nm). Small droplets reduce amount of solvent impurities that adhere to the dried particles

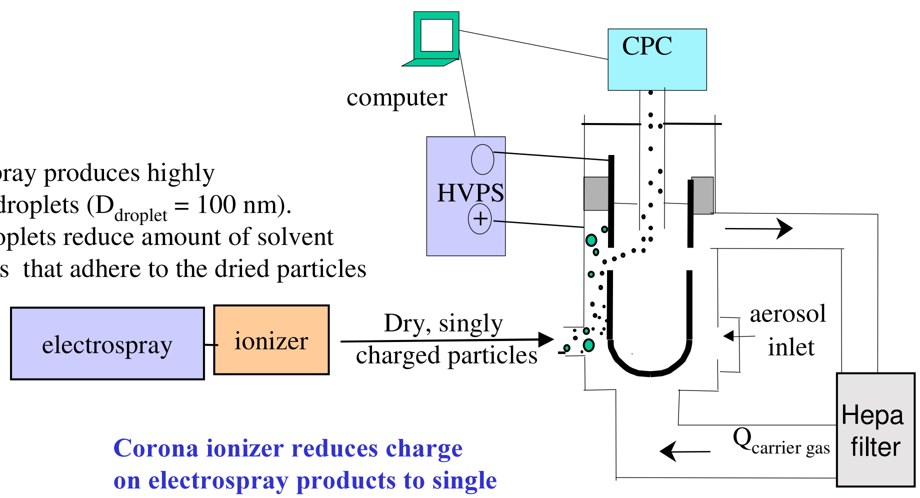

Corona ionizer reduces charge on electrospray products to single

CPC with high sensitivity to d<3 nm particles[3]
(Commercial CPCs are insensitive below 3 nm)

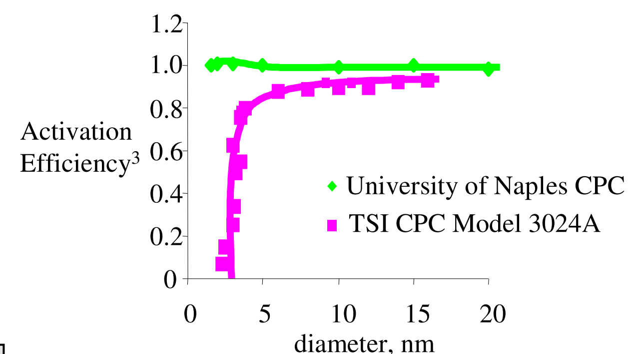

Electrostatic classifier passes particles according to their size to the detector. We modified to allow high carrier gas flow – reducing diffusional peak broadening and losses.

Example of size determination with E-DMA : Macromolecule Lysozyme

Molecular clusters of Lysozyme

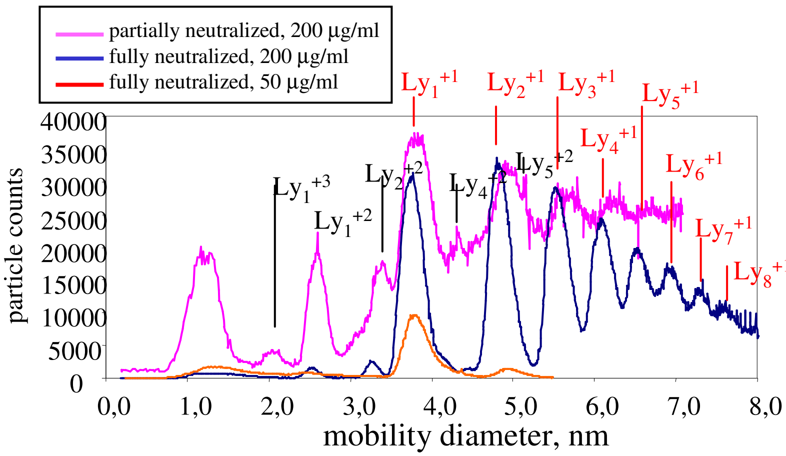

<50 µg/ml (one molecule per drop) gives single Ly_1^{+1} peak

peak is proportional to concentration in solution

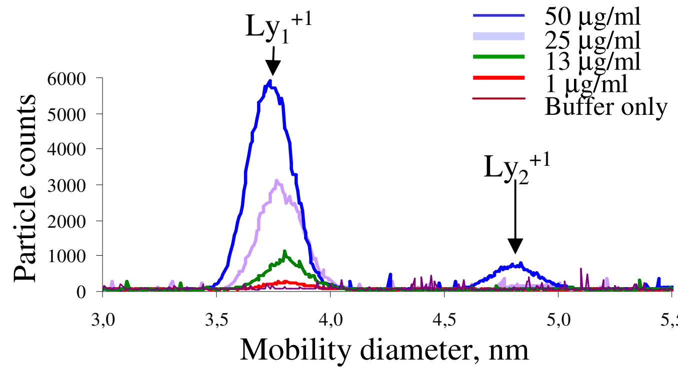

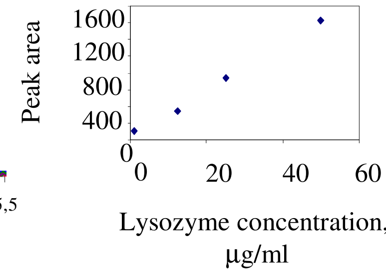

Measured Electrical Mobility, Z, of singly charged Lysozyme clusters

Diameter[4], calculated from measured Z

$$d = \left(\frac{0.441 q (kT/m)^{0.5}}{pZ} \right)^{0.5}$$

d='mobility' diameter – not accounting for 'effective diameter' of carrier gas
n=number of molecules in cluster
M=molecular weight of molecule
NA=Avagadro's number
ρ=density
Q=charge
K=Boltzmann constant
t, p=temperature, pressure of carrier gas
Z=electrical mobility

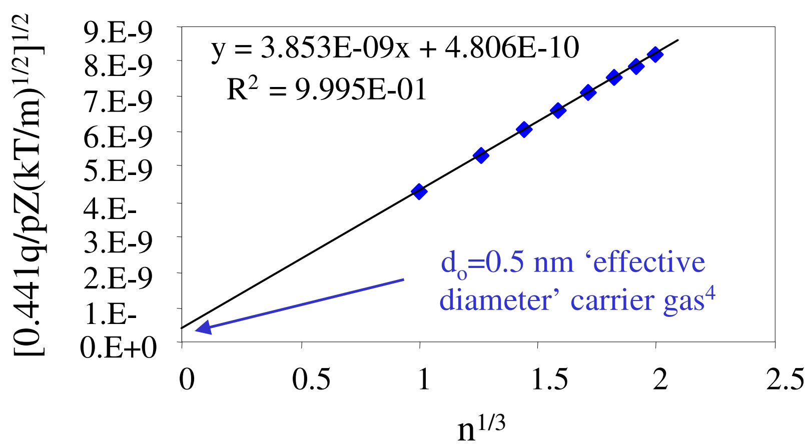

Diameter, calculated from known mass

$$d = \left(\frac{6nM}{N_A \rho \pi} \right)^{\frac{1}{3}}$$

Calculating Adhesion Efficiency of nanoparticles (or macromolecules) within the framework of Gas Kinetic Theory (GKT)

N_i = gas phase particle density
m_i = particle mass
i= particle size

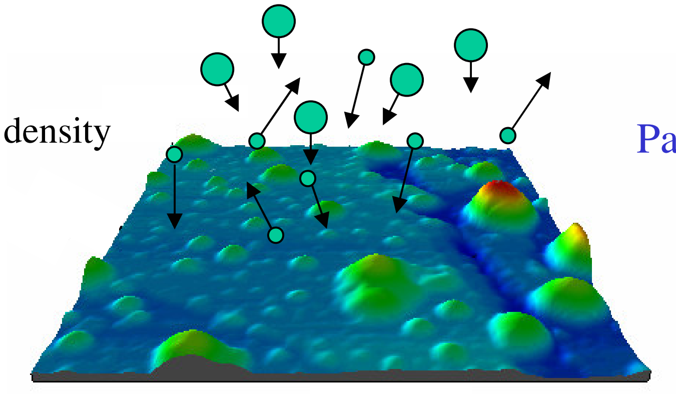

Particles that 'bounce' are not counted by AFM

Adhered particles are counted by AFM

Adhesion velocity[5], $a_i = \frac{\text{fraction of collisions with kinetic energy < Interaction potential well}}{\text{time * surface}}$

Adhesion efficiency, γ

$$\gamma = \left(1+\frac{\Phi_0}{kT}\right)e^{\left(-\frac{\Phi_0}{kT}\right)}$$

$$a_i = \frac{N_i}{4\pi}\int_0^{v_0} v f(v)dv \int_0^{\pi/2}\cos\vartheta\sin\vartheta d\vartheta \int_0^{2\pi} d\varphi = \frac{\left(\frac{8kT}{\pi m_i}\right)^{0.5}}{4}\gamma N_i$$

Speed of kinetic energy value Φ_o (minimum of interaction potential), $v_0 = (2\Phi_0(1/m_i))^{0.5}$

<u>**Assumptions**</u>
- Velocity distribution function is Maxwell-Bolzmann
- Interactions between particles and AFM substrate can be modeled by a Lennard-Jones 6-12 potential, Φ_r
- Hamaker[6] constant for nanoparticles = $5*10^{-21}$ for soot=$2*10^{-20}$ J *(soot is more graphitic with higher polarizability)*
- Particles are spherical with a density of 1 g/cm^3

The same modeling approach successfully explains the lower coagulation rate of nanoparticles than soot in flames. [7]

Adhesion & Coagulation efficiency increases 3 orders of magnitude as a function of size from the smallest nanoparticle to primary soot particles[7]

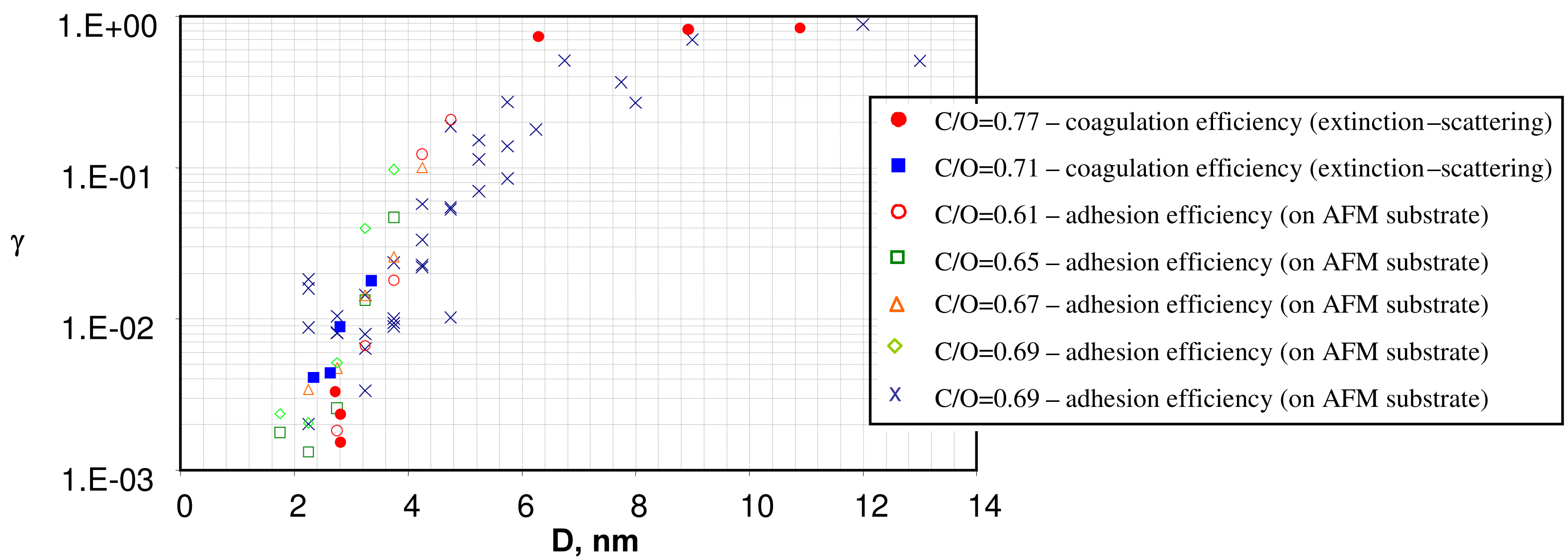

Size distribution accounting for size-dependent adhesion efficiency

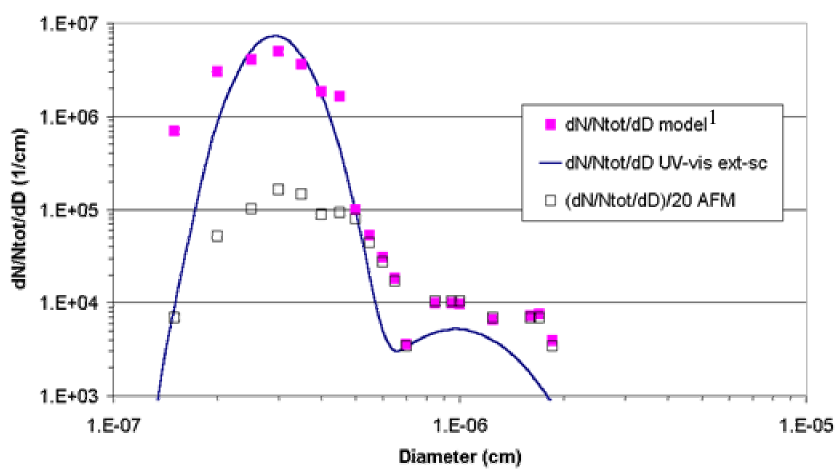

[1] N_i is calculated by the model through a_i obtained from AFM measurement

Extinction Spectrum of Air-diluited (10:1) Exhausts from a Diesel and a Spark-ignited (Gasoline) Car Driven at Chassis Dynamometer - 50 km/h

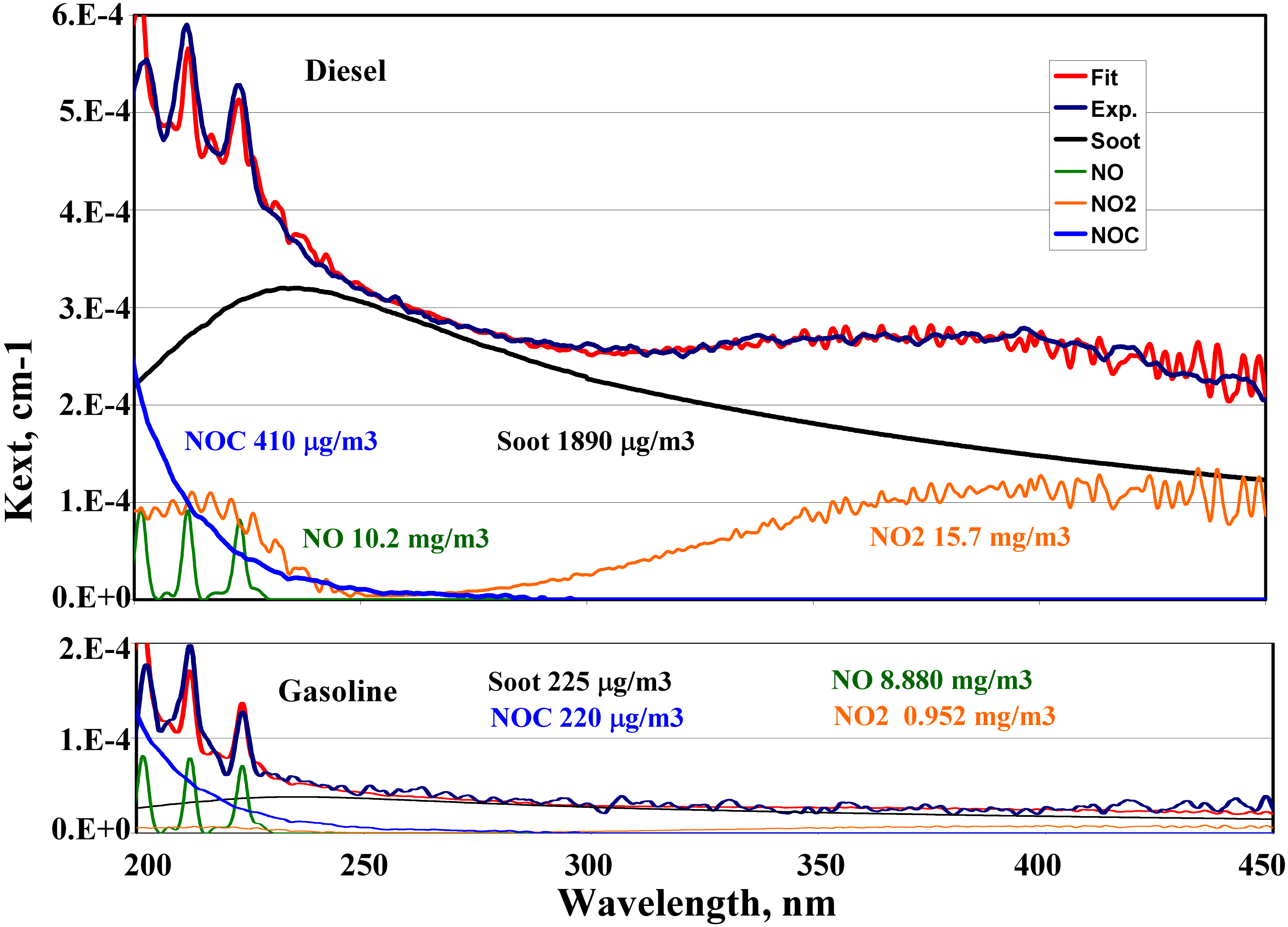

NOC and Soot size distributions for various engines and operating conditions

Concentration of Soot and NOC – UV-vis extinction measurements

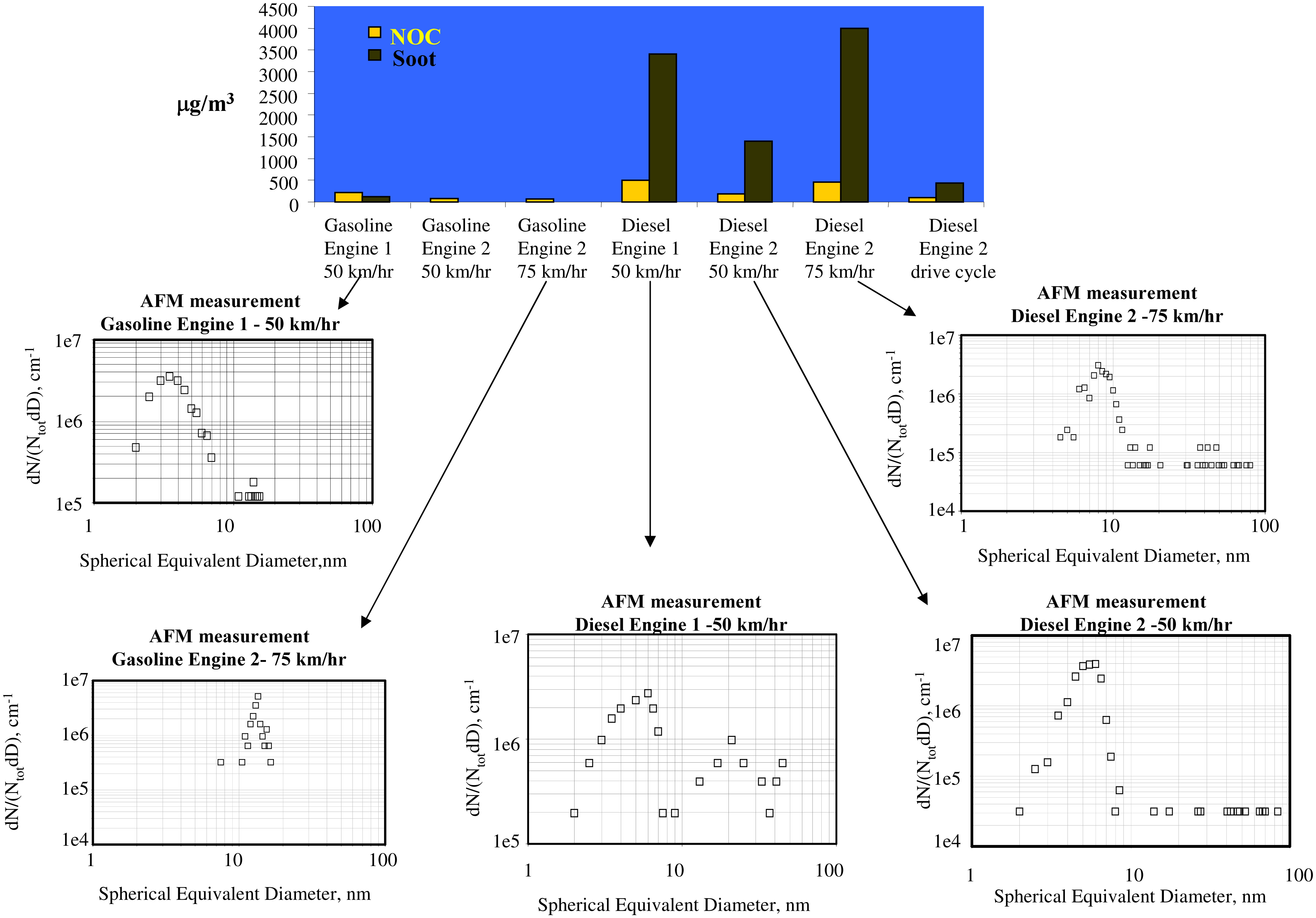

Total Organic Carbon (TOC) measurement and NOC concentration in water samples

Total Organic Carbon (TOC) Measurements

Total organic carbon (TOC) concentration was measured with a Shimadzu TOC-5000A Analyzer. After sparging with high purity oxygen for several minutes to remove CO and CO_2 in the water samples, the sample is burned in a catalytic combustion tube and then measures CO_2 with a non-dispersive infrared gas analyzer.

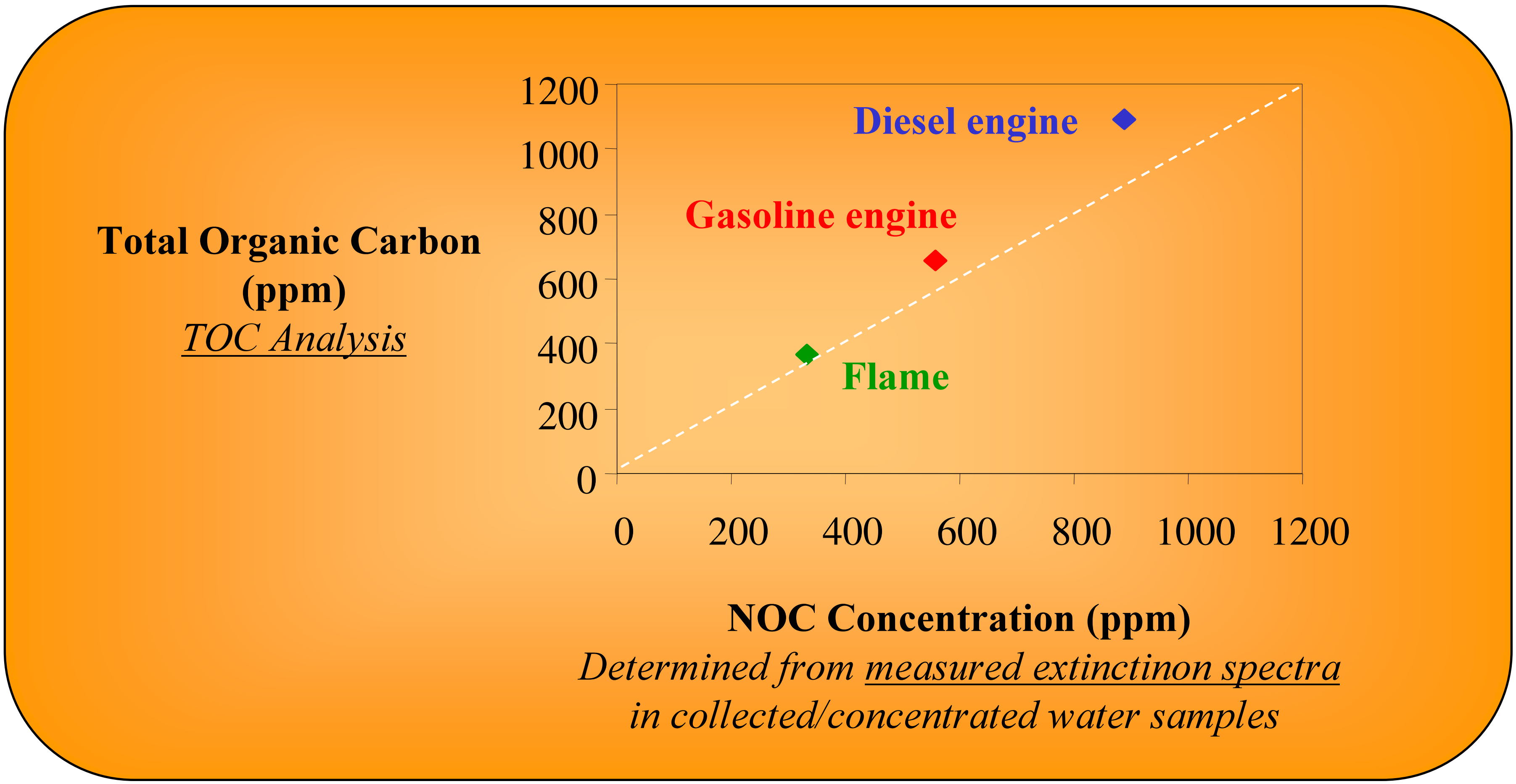

Comparing volume fraction of $\frac{f_v(NOC)}{f_v(Soot)}$ *in Water Samples, on AFM Substrates, and In Situ*

Test vehicle – dynamometer conditions	$\dfrac{\left(\frac{f_v(NOC)}{f_v(soot)}\right)K_{ext}\ \text{(water sample)}}{\left(\frac{f_v(NOC)}{f_v(soot)}\right)K_{ext}\ \text{(gas phase)}}$	$\dfrac{\left(\frac{f_v(NOC)}{f_v(soot)}\right)\ \text{AFM (on substrate)}}{\left(\frac{f_v(NOC)}{f_v(soot)}\right)K_{ext}\ \text{(gas phase)}}$
1-gasoline - 50 km/hr	5.5	0.2
2-gasoline -50 km/hr	Indetectable Soot Concentration by Extinction (< 100 μg/m^3)	Indetectable Soot Concentration by Extinction (< 100 μg/m^3)
2-gasoline - 75 km/hr	Indetectable Soot Concentration by Extinction (< 100 μg/m^3)	Indetectable Soot Concentration by Extinction (< 100 μg/m^3)
1-diesel-50 km/hr	113	0.016
2-diesel-50 km/hr	122	0.16
2-diesel-75 km/hr	41	0.31
2-diesel-integrated cycle	20	Did not take AFM measurements

Collection efficiency of NOC in water samples (2-diesel-integrated cycle) = $\dfrac{K_{ext,\,NOC}\ \text{(measured in water collected from heat exchanger)}}{K_{ext,\,NOC}\ \text{(measured in diluted exhaust with heat exchanger off)} - K_{ext,\,NOC}\ \text{(measured in diluted exhaust with heat exchanger on collecting water sample)}}$ = 60%

Size Distribution of Particles in Water Samples Collected from Engine Exhausts
Vehicles Driven by Dynamometer – Cummulative Sampling – New European Drive Cycle (NEDC)

Difference between hydrodynamic diameter (measured by DLS) and mobility diameter (measured in E-DMA) may be related to solvation state or particle – water interactions

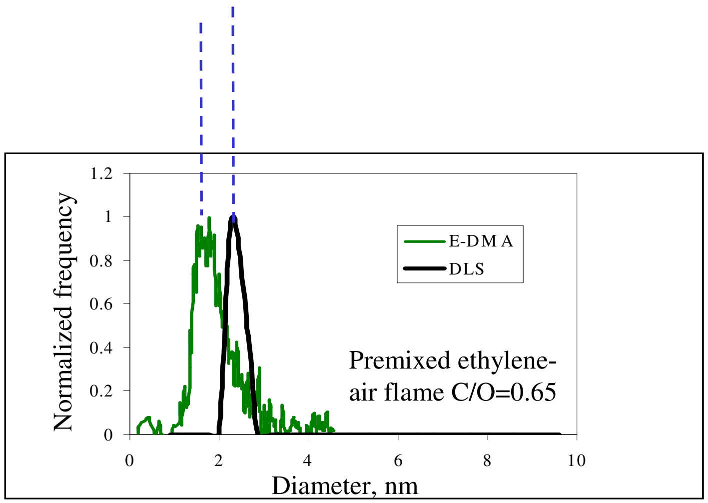

Dynamic Light Scattering, DLS

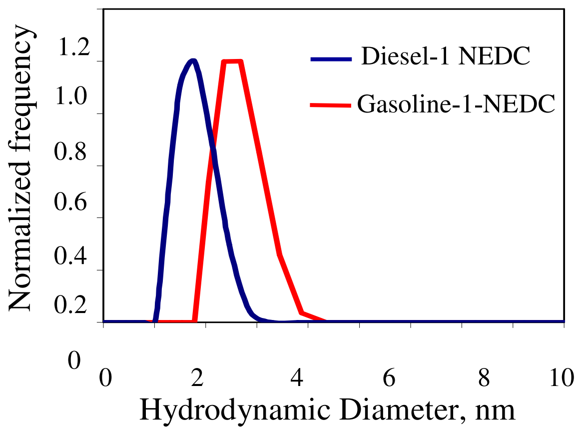

Electrospray-Differential Mobility Analysis, E-DMA

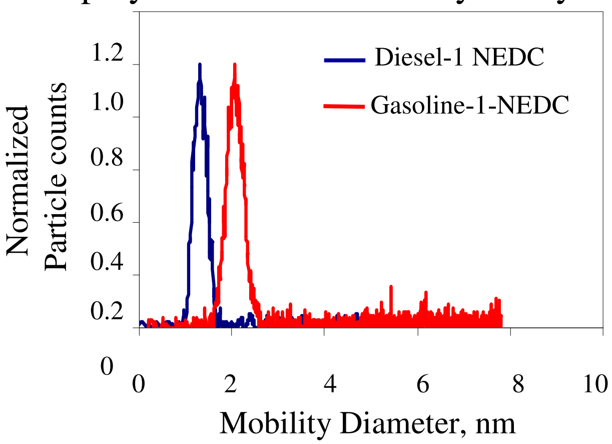

Conclusions

•We measured particles in laboratory premixed ethylene-air flames and 4 last generation vehicles.

•Diesel exhausts contained bimodal size distributions determined by atomic force microscopy (AFM) and UV-vis extinction spectroscopy

➢Size distributions are similar for different vehicles and driving conditions

•Gasoline engine exhausts contained mainly Nanosized Organic Carbon (NOC) particles observed by UV-visible extinction spectroscopy, and AFM measurements show that the particle size distribution is unimodal.

➢The mean nanoparticle size varied for different cars.

•The adhesion efficiency on AFM substrates of the smallest nanoparticles is 3 orders of magnitude lower than for soot in flames.

•The modeling approach within the framework of the Gas Kinetic Theory describes well the widely different behaviors of nanoparticles and soot, both for particle coagulation and for adhesion to surfaces

•Collection of particles in water samples preferably captures the smaller mode NOC particles, accounting for 75 – 90% of total organic carbon (TOC).

•The size of NOC particles collected in water samples using electrospray – differential mobility analysis and dynamic light scattering is smaller than those measured by AFM .

References

[1]A. Borghese and S. Merola, 'Detection of extremely fine carbonaceous particles in the exhausts of diesel and spark-ignited internal combustion engines by means of broad-band extinction and scattering spectroscopy in the ultraviolet band 190 nm – 400 nm', Prod. Comb. Inst. Vol. 27:2101-2109.

[2] L. A. Sgro, G. Basile, A. C. Barone, A. D'Anna, P. Minutolo, A. Borghese, A. D'Alessio 'Detection of combustion formed nanoparticles', Chmosphere Vol. 51: 1079-1090, 2003.

[3] L. A. Sgro and J. Fernández de la Mora, 'A simple design for a turbulent mixing CNC for charged particle detection down to 1.2 nm', J. Aerosol Sci. Vol. 38: 1-11, 2004. C.S. Kim, K. Okuyama, J. Fernández de la Mora, 'Performance Evaluation of an improved particle size magnifier for single nanoparticle detection,' Aerosol Sci. Vol. 34: 791-803, 2003.

[4] J. Fernández de la Mora, L. de Juan, K. Liedtke, A. Schmidt-Ott, 'Mass and size determination of nanometer particles by means of mobility analysis and focused impaction', J. Aerosol Sci. Vol. 34: 79-98, 2003.

[5] Mc Quarrie and J.D. Simon, Physical Chemistry: A Molecular Approach, Univ. Sci. Books, 1997.

[6]G. Narsimhan, and E. Ruckenstein, 'The Brownian Coagulation of aerosols over the entire range of Knudsen numbers: connection between the sticking probability and the interaction forces,' J. Colloid and Interface Science, Vol. 104, No. 2, 1985.

[7]D'Alessio, A., Barone, A. C., Cau, R., D'Anna, A., Minutolo, P. 'Surface deposoition and coagulation efficiency of combustion generated nanoparticles in the size range from 1 nm to 10 nm', 3oth Intl. Symp. Comb. Inst., Chicago, July 25-30, 2004.

[8]A. Borghese and S. Meroa, 'Detection of extremely fine carbonaceous particles in the exhausts of diesel and spark-ignited internal combustion engines by means of broad-band extinction and scattering spectroscopy in the ultraviolet band 190 nm – 400 nm', Prod. Comb. Inst. Vol. 27:2101-2109.

[9]A.C. Barone, A. D'Alessio, A. D'Anna, 'Morphological characteristization of the early process of soot formation by atomic force microscopy,' Comb. Flame 132: 181-187.